SUPPLEMENTARY INFORMATION

Table S1: Interatomic potential model used for bulk and surface calculations.

a) Two-body

Interaction	A (eV)	ρ(Å)	C (eV.Å^6)	Y (e)	K (eV.Å^{-2})
Li^+ - O^{2-}	632.1010	0.2906	0.0	1.0	99999.0
Fe^{2+} - O^{2-}	1105.2409	0.3106	0.0	2.997	19.26
P^{5+} - O^{2-}	897.2648	0.3577	0.0	5.0	99999.0
O^{2-} - O^{2-}	22764.3	0.149	44.53	-2.96	65.0

b) Three-body

Bonds	k (eVrad^{-2})	θ_0 (^{o})
O^{2-} - P^{5+} - O^{2-}	1.322626	109.47

Table S2: Properties for all crystal planes and cuts examined in this study.

Plane	Tasker surface type	*d*-spacing, d_{hkl} (Å)	Surface energy, $E_{surface}$ / J.m^{-2}		Attachment energy, E_{attach} / J.m^{-2}
			Unrelaxed	Relaxed	
(002)	III	2.33	2.40	1.11	-11.18
(002)	II	" "	3.21	1.20	-18.21
(020)	III	3.01	1.64	0.72	-5.74
(020)	II	" "	3.94	1.06	-6.49
(200)	III	5.19	2.12	0.87	-3.39
(200)	II	" "	2.37	1.05	-3.65
(011)	III	3.69	2.55	0.75	-6.43
(011)	II	" "	5.26	1.21	-11.84
(024)	II	1.09	4.50	1.02	-51.28
(024)	III	" "	3.38	1.07	-28.28
(024)	III	" "	3.38	1.04	-27.31
(042)	II	1.27	2.41	0.82	-18.03
(042)	III	" "	3.99	0.88	-36.59
(042)	III	" "	3.99	1.06	-52.32
(101)	III	4.26	2.51	1.10	-4.74
(101)	III	" "	2.51	1.02	-4.69
(101)	III	" "	1.65	0.88	-3.43
(101)	III	" "	1.65	0.89	-3.42
(101)	II	" "	4.22	1.49	-7.65
(102)	II	" "	3.72	1.17	-20.28
(102)	III	2.28	3.29	1.15	-19.85
(102)	II	" "	3.72	1.24	-27.02
(102)	III	" "	5.42	1.39	-38.77
(220)	III	2.60	6.07	1.22	-22.45
(220)	III	" "	6.07	1.22	-26.20

(220)	II	“ ”	3.62	0.92	-16.25
(111)	III	3.48	2.94	1.05	-7.60
(111)	III	“ ”	2.94	0.89	-6.81
(111)	III	“ ”	2.24	1.00	-5.34
(111)	III	“ ”	2.24	1.04	-5.55
(112)	III	2.13	3.77	1.09	-20.11
(112)	III	“ ”	3.77	0.90	-16.81
(112)	II	“ ”	4.69	1.28	-24.53
(112)	III	“ ”	2.57	0.96	-22.55
(112)	III	“ ”	4.42	0.93	-21.69
(112)	III	“ ”	4.42	1.00	-24.15
(112)	III	“ ”	2.57	0.88	-20.22
(112	III	“ ”	4.69	1.03	-19.10
(240)	III	1.45	3.53	0.96	-21.95
(240)	III	“ ”	3.53	0.86	-17.43
(240)	II	“ ”	5.55	1.19	-34.50
(121)	II	2.46	2.44	0.94	-11.27
(121)	III	“ ”	5.14	1.31	-18.56
(121)	III	“ ”	5.14	1.07	-19.92
(121)	III	“ ”	5.09	1.23	-20.12
(121)	III	“ ”	5.09	1.09	-18.49
(121)	III	“ ”	5.13	1.09	-18.84
(121)	III	“ ”	5.13	1.22	-21.54
(122)	III	1.82	7.45	1.01	-53.51
(122)	III	“ ”	7.45	0.90	-72.61
(122)	II	“ ”	3.81	0.97	-25.03
(122)	III	“ ”	2.65	0.92	-14.17
(122)	III	“ ”	2.65	0.80	-15.74
(122)	II	“ ”	3.81	1.02	-24.98

(201)	III	3.47	1.37	0.71	-4.27
(201)	II	“ ”	6.14	1.72	-16.38
(201)	III	“ ”	2.36	0.90	-6.26
(201)	II	“ ”	6.14	1.28	-14.32
(210)	III	3.93	2.61	0.90	-5.55
(210)	III	“ ”	5.50	1.39	-12.26
(211)	III	3.01	2.51	0.87	-8.60
(211)	III	“ ”	2.51	0.80	-8.67
(211)	II	“ ”	3.27	1.06	-9.64
(211)	III	“ ”	3.83	1.00	-11.40
(211)	III	“ ”	3.83	1.04	-10.04
(211)	II	“ ”	3.27	0.99	-10.29
(212)	III	2.01	5.98	0.98	-29.02
(212)	III	“ ”	5.98	1.49	-36.42
(212)	III	“ ”	2.70	1.06	-12.12
(212)	III	“ ”	2.26	0.86	-11.60
(221)	III	2.27	3.38	1.02	-17.61
(221)	III	“ ”	3.38	0.93	-17.50
(221)	II	“ ”	2.52	0.79	-10.69
(221)	II	“ ”	2.52	0.85	-11.84
(221)	III	“ ”	2.70	0.89	-14.83
(221)	III	“ ”	2.70	1.06	-16.40

Notes on Surface Construction

(a) Identification of F faces

In determining the Periodic Boundary Chains (PBCs), the phosphate ions were treated as point charges centred on the P^{5+} position. When this is done, four different PBCs can be described, viz. [001], [010], [100], [101] and [-101], as shown in Figure S1. The F faces of Hartman-Perdok theory are then found to be {002}, {020}, {200}, {011}, {101}, and {220}. Of these, {020} has the strongest F face character, with PBCs perfectly parallel to the surface plane, whereas for all other faces the PBCs weave in and out of the parallel plane, the chains becoming more tortuous as the number of non-zero indices increases.

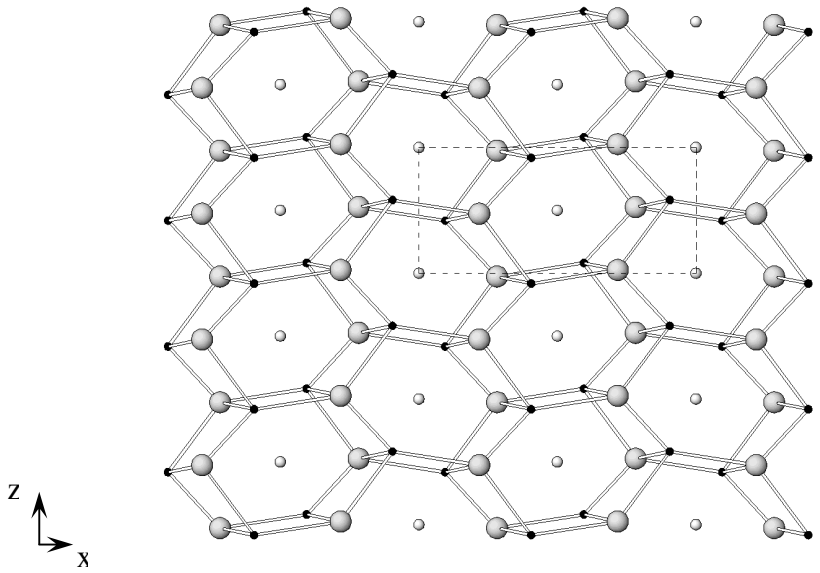

Figure S1. Periodic Bond Chains (PBCs) between Fe ions (large grey spheres) and P ions (small black spheres) in orthorhombic $LiFePO_4$. Li ions sit in the large channels. A unit cell is shown with dashed lines.

(b) Arrangement of Li ions

For many surfaces, the Li^+ ions are aligned along the long axis of the 2D (surface) cell. An alternative arrangement is to have the ions in a zig-zag configuration by doubling the cell down the short axis, *i.e.*,

creating a [2x1] cell. (Theoretically, an infinite number of configurations and rearrangements of the ions in the surface layer of Type III surfaces can be created by increasing the size of the surface cell beyond [1x1].) For (010) and (120) surfaces, this zig-zag arrangement was found to give surface and attachment energies slightly lower than the [1x1] surface. For example, in the case of (010) [2x1] with the Li^+ ions in the terminating layer arranged in a zig-zag fashion, the surface energy decreased from 0.75 to 0.72 J/m^2. In the real material, under normal conditions it might be expected that the Li^+ ions and vacancies will be randomly distributed over possible sites, particularly if insertion or deinsertion from the Li-ion conducting electrolyte is taking place.

For many of the crystal planes examined there are two distinct Type II slice configurations, separated by half a slice thickness d_{hkl}, with a corresponding number of Type III configurations at different shifts. For (101) and (121), only one Type II surface exists, whereas for (010), (011), (111), (210) and (212) planes, only Type III surfaces can be formed.

(c) High symmetry surfaces

In the case of index forms (001), (010), (100), (110), (012), (021) and (120), the pairs of surfaces obtained by slicing the crystal at intervals of 0.5 lattice spacings, whether Type II or Type III, are symmetrically-equivalent on account of the two-fold screw axes in space group *Pnma*. In these cases the growth slices have a thickness of half d_{hkl}, and contain only two formula units rather than the four formula units of lower symmetry surfaces.

In the case of (012), (021) and (102) surfaces, Type II and Type III surfaces have very similar surface (and attachment) energies to each other. For these crystal orientations it is possible that growth occurs via both surfaces, separated by steps equal to a submultiple of the slice thickness d_{hkl}. The reduced thickness of the growth slice may mean that growth in these directions may occur more rapidly than the relative attachment energies of a single slice would suggest.